Supporting Information Available

Nanomechanical properties of TiO_2 granular thin films

Ms. Ref. No.: am-2010-00455q

Houman Yaghoubi[1, 5], *Nima Taghavinia*[2, 3]*, *Eskandar Keshavarz Alamdari*[1, 4], *Alex A. Volinsky*[5]

[1] New Materials Department, Materials and Energy Research Center (MERC), P.O. Box 14155-4777, Tehran, Iran

[2] Physics Department, Sharif University of Technology, Tehran 14588, Iran

[3] Institute for Nanoscience and Nanotechnology, Sharif University of Technology, Tehran 14588, Iran

[4] Department of Mining and Metallurgical Engineering, Amirkabir University of Technology, 424 Hafez Avenue, P.O. Box 15875-4413, Tehran, Iran

[5] Department of Mechanical Engineering, University of South Florida, Tampa, FL 33620, USA

*Corresponding author: Fax: +98-(21)-66164532, E-mail: taghavinia@sharif.edu

E-mail addresses: Yaghoubi.houman@gmail.com (H. Yaghoubi), Taghavinia@sharif.edu (N. Taghavinia), alamdari@aut.ac.ir (E. K. Alamdari), volinsky@usf.edu (A. A. Volinsky)

Table S1. Numerical data for nanoindentation tests of TiO_2 layers on glass annealed between 100 ^{o}C and 500 ^{o}C.

Temp. (°C)	Load (μN)	Max. Force (μN)	Max. Depth h_{max} (nm)	Contact Depth (nm)	Contact Stiffness (μN/nm)	H (GPa)	E_r (GPa)	Contact Area (nm^2)	Power-law coefficients $P=A(h-h_f)^m$		
									A	h_f	M
100	125	112.5	78.2	73.3	38.0	0.42	9.5	2.672E+5	4.048	69.82	1.915
200	125	114.0	66.0	61.0	35.1	0.58	10.3	1.955E+5	2.477	56.89	2.031
300	125	114.8	60.9	56.8	34.1	0.69	10.6	1.731E+5	3.835	53.06	1.855
400	125	113.2	71.1	66.9	35.7	0.50	9.7	2.283E+5	4.176	63.36	1.860
500	125	114.1	73.1	68.8	33.2	0.49	9.6	2.396E+5	3.528	64.93	1.869

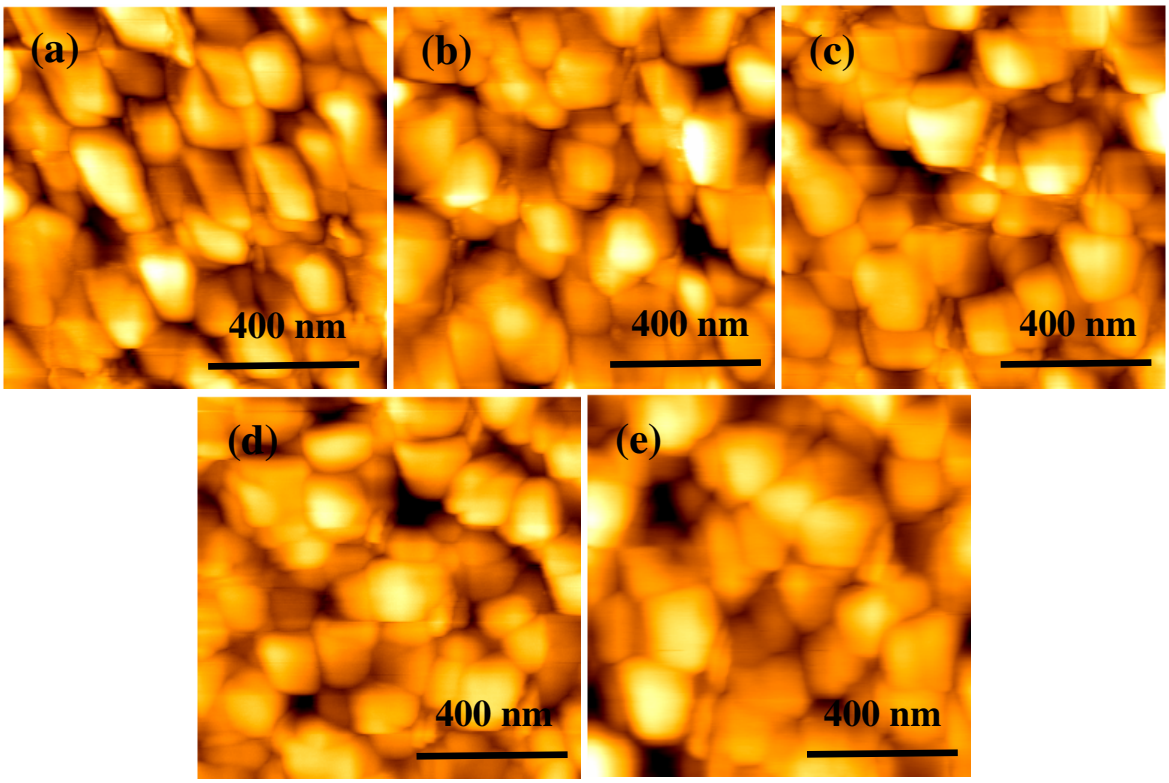

Figure S1. Surface morphology of TiO_2 films annealed at: (a) 100 °C, (b) 200 °C, (c) 300 °C, (d) 400 °C and (e) 500 °C.

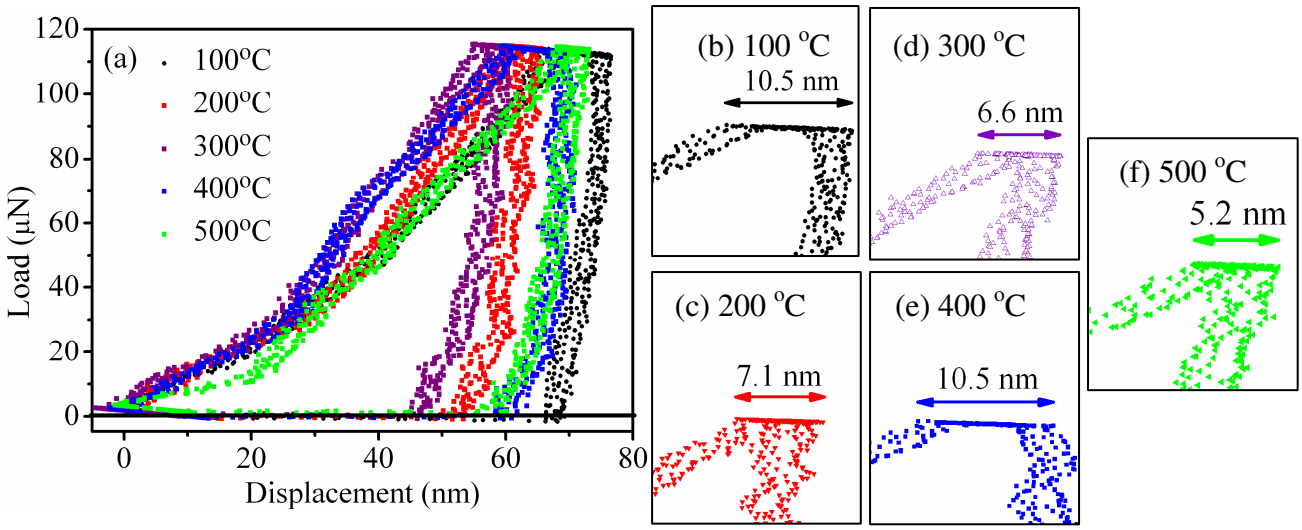

Figure S2. (a) Typical load-displacement curves for the TiO_2 films annealed between 100 °C and 500 °C; (b-f) displacement during hold time (creep) for films annealed between 100 °C and 500 °C.

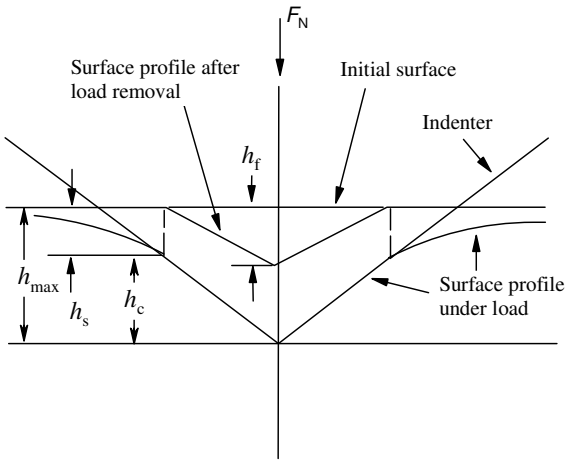

Figure S3. Assumed contact geometry with definition of h_{max} under load and h_f as the final depth of the impression after unloading (contact geometry under load and after unloading).

Figure S3 provides a better view of the mentioned parameters and depicts assumed contact geometry under load and after unloading.

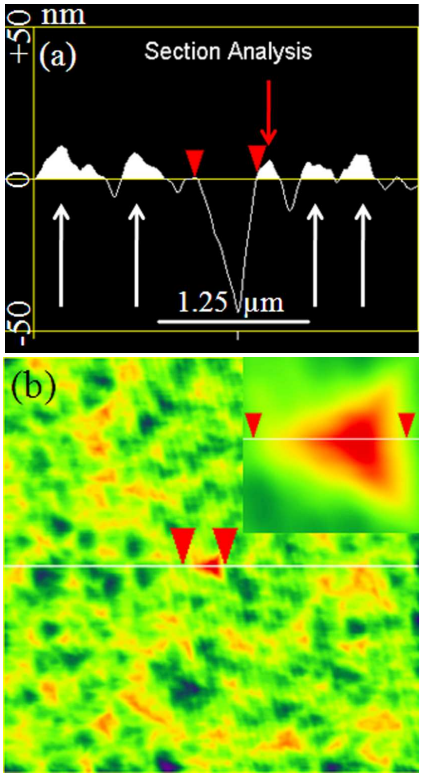

Figure S4. (a) Section analysis and (b) corresponding AFM image of the 125 µN indent of the TiO_2 film annealed at 100 ^oC.

AFM images and the corresponding section analysis plots of a 125 μN indent on the 100 ^{o}C annealed sample are presented in Figure S4 (a, b). Figure S4 clearly shows that there is no pile-up or sink-in at the edges of the residual indent. This statement is also true for the films annealed between 200 ^{o}C and 500 ^{o}C. White hump seen at the right edge of residual indent in Figure S4a is the roughness artifacts and should not be regarded as the pile-up effect, since similar humps are present in portions of the section profile far from the indent. The average height of these humps is about 12 nm, similar to AFM topographical images.

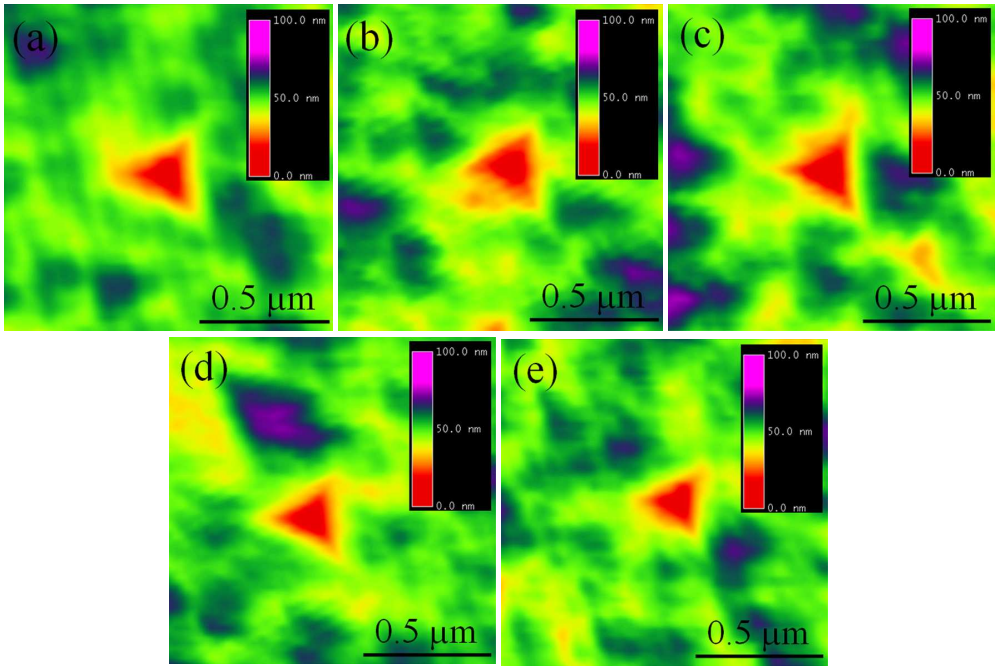

Figure S5. Selection of AFM images of the residual indents on the TiO_2 films annealed at (a) 100 ^{o}C, (b) 200 ^{o}C, (c) 300 ^{o}C, (d) 400 ^{o}C and (e) 500 ^{o}C.

To obtain a precise picture of what is really happening under indentation residual indentations were imaged for better quantification of nanoindentation results, i.e. pile up and/or sink-in effects and elastic/plastic behavior. Figure S5 shows AFM images of select 125 μN residual indents in TiO_2 films annealed between 100 ^{o}C and 500 ^{o}C. Indentation images evidently confirm plastic nature of the TiO_2 films' deformation and/or contact.

Images in Figure S5 correspond to load-displacement curves in the paper (Figure. 2). Moreover, no pile up and sink-in effects are observed.

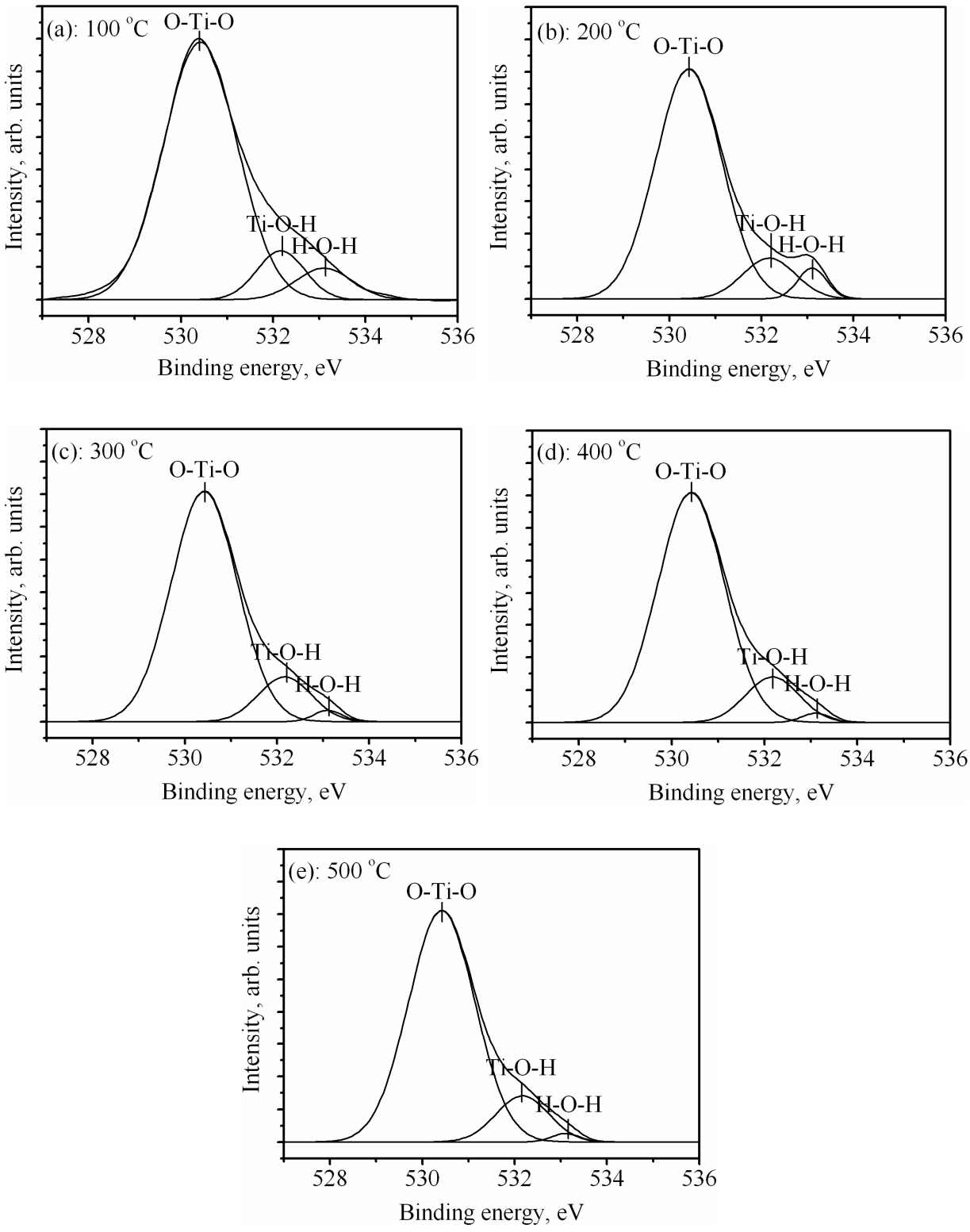

Figure S6. (a-e) XPS spectra of the O 1s region for the samples annealed between 100 °C and 500 °C.

In order to determine film scratch resistance at constant normal force, three approaches have been undertaken based on: 1. The volume of the excavated ditch (the scratch

volume) [47] or the scratch area, 2. The scratch depth [78] and 3. The friction coefficient along the scratch length [79]. The volume of the excavated ditch and the scratch area can be measured using the AFM images with the section analysis. Residual depth measurements can be performed from a transverse profile section of a nanoscratch groove. The friction coefficient as a measure of the resistance to abrasion is calculated as the ratio of the lateral force over the normal force along the whole scratch length.

Nanoscratch experiments were performed at constant normal force and produced 4 µm scratches. Figure S7 (a) shows the 3D AFM image of the residual scratch on the 100 ^{o}C annealed sample. The volume and the depth of excavated trenches were measured as a function of annealing temperature. The results clearly show decreasing trend of the volume and the depth of scratches with increasing annealing temperature (Figure S7 (b)). The volume of excavated trenches for layers annealed between 100 ^{o}C and 500 ^{o}C was 2.31×10^{-2} µm^3, 2.03×10^{-2} µm^3, 1.2×10^{-2} µm^3, 1.03×10^{-2} µm^3 and 0.97×10^{-2} µm^3, respectively. Moreover, the maximum scratch depth reached 31.6 nm for 100 ^{o}C annealed sample, and only 18.7 nm for 500 ^{o}C, while no significant improvement was observed after 300 ^{o}C annealing. Variation of the friction coefficient vs. temperature along the scratch length was evaluated for all samples (Figure S9). Based on these results, the variation was not reproducible or ordered.

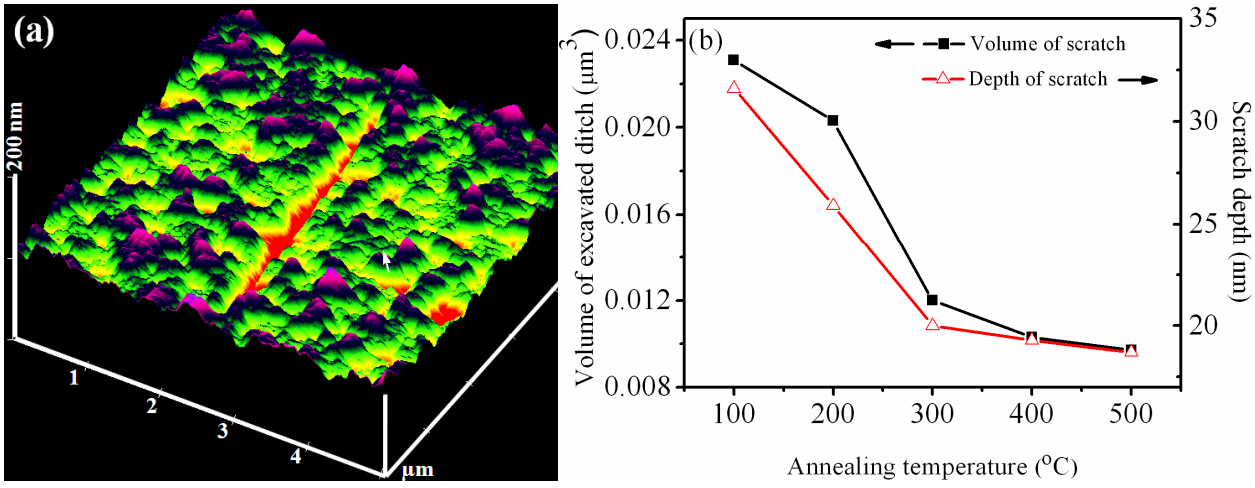

Figure S7. (a) 3D AFM image of the residual scratch on 100 ^{o}C annealed layer, (b) variation of the excavated trench volume and the scratch depth vs. annealing temperature.

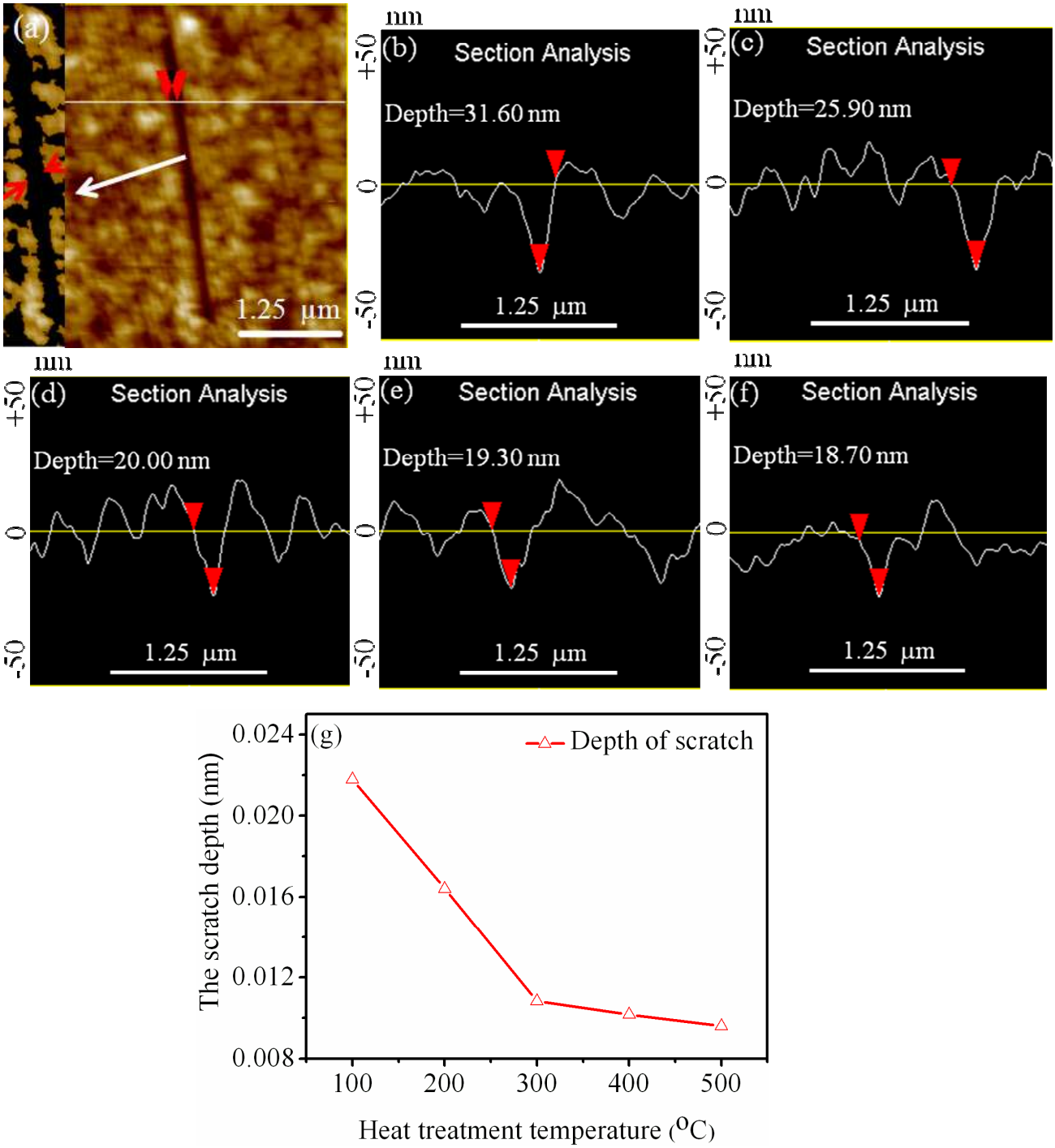

Figure S8. (a) 2D AFM images of a nanoscratch on 100 °C annealed sample; residual depth measurements from transverse section profiles of nanoscratch grooves for (b) 100 °C, (c) 200 °C, (d) 300 °C, (e) 400 °C and (f) 500 °C annealed samples and (g) variation of the scratch depth vs. annealing temperature.

Figure S8 shows a scratch track appearance for the TiO_2 film annealed at 100 °C and section profiles of nanoscratch grooves for samples annealed between 100 °C and 500 °C. Figure S8 (f) clearly displays a shallow wear (scratch) track surface (residual depth of scratch

groove is ~ 18.7 nm), whereas Figure S8 (b) shows a deeper wear (scratch) track surface (residual depth of scratch groove is ~ 31.6 nm). Please note that Figure S8 (g) demonstrates no significant improvement observed after 300 ^{o}C annealing with respect to the scratch resistance.

Figure S8 (a) shows no pile-up effects at the edges of residual nanoscratch imprint, and section analyses also confirm this statement. The humps which occasionally can be seen at the edges of residual scratches are observable at different parts along the scratch length and actually are the roughness artifacts and are not attributed to the pile-up effect.

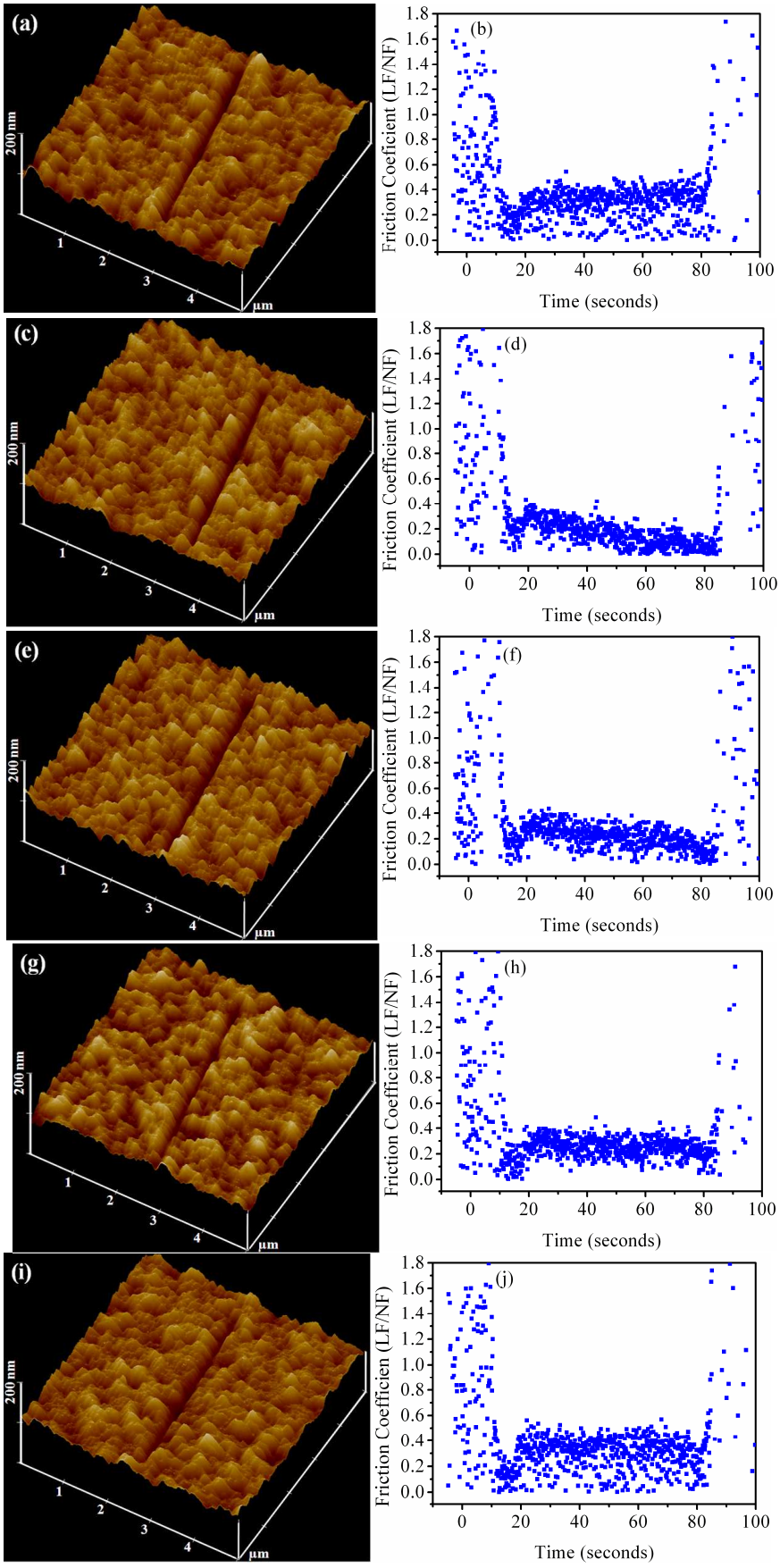
(a)
200 nm
1
2
3
4
µm
(b)
Friction Coefficient (LF/NF)
Time (seconds)
(c)
(d)
(e)
(f)
(g)
(h)
(i)
(j)
Friction Coefficien (LF/NF)

Figure S9. AFM images of residual scratches and variation of the friction coefficient vs. time for layers annealed at (a) 100 °C, (b) 200 °C, (c) 300 °C, (d) 400 °C, (e) 500 °C.

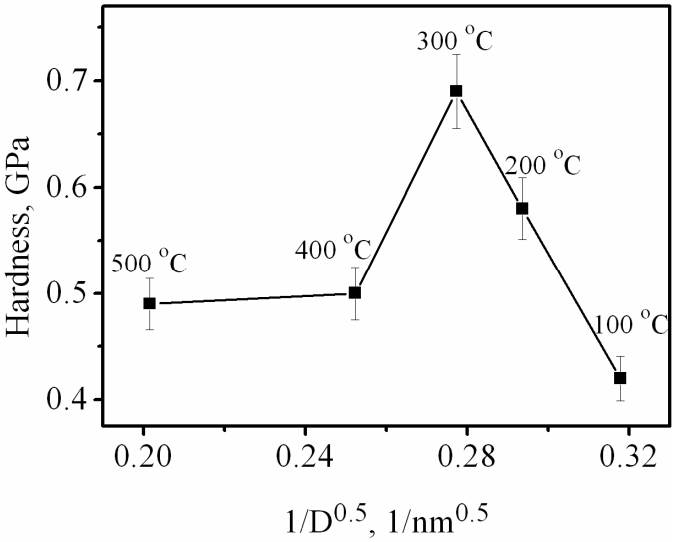

Figure S10. Hall-Petch plot for TiO_2/Glass (hardness as a function of $1/D^{0.5}$).

In order to verify the validity of Hall-Petch equation, the measured hardness values for samples heat treated between 100 °C and 500 °C, were plotted against $D^{-0.5}$ (Figure S10), where D is the grain size estimated from the XRD peak broadening (as indicated in Figure 7). The first data point with the lowest $D^{-0.5}$ value corresponds to 500 °C, and the last one corresponds to 100 °C annealing. The increase in hardness from 100 °C to 300 °C annealed films (the last 3 points) is due to the removal of water from the film, leading to condensation reactions that provide stronger binding of neighboring particles. The decrease in hardness for 300 °C to 500 °C annealed films (the first 3 points) is in direction of Hall-Petch prediction, however, it does not show a linear dependence, that is, the Hall-Petch equation cannot explain the decrease in hardness and modulus after 300 °C annealing temperature.

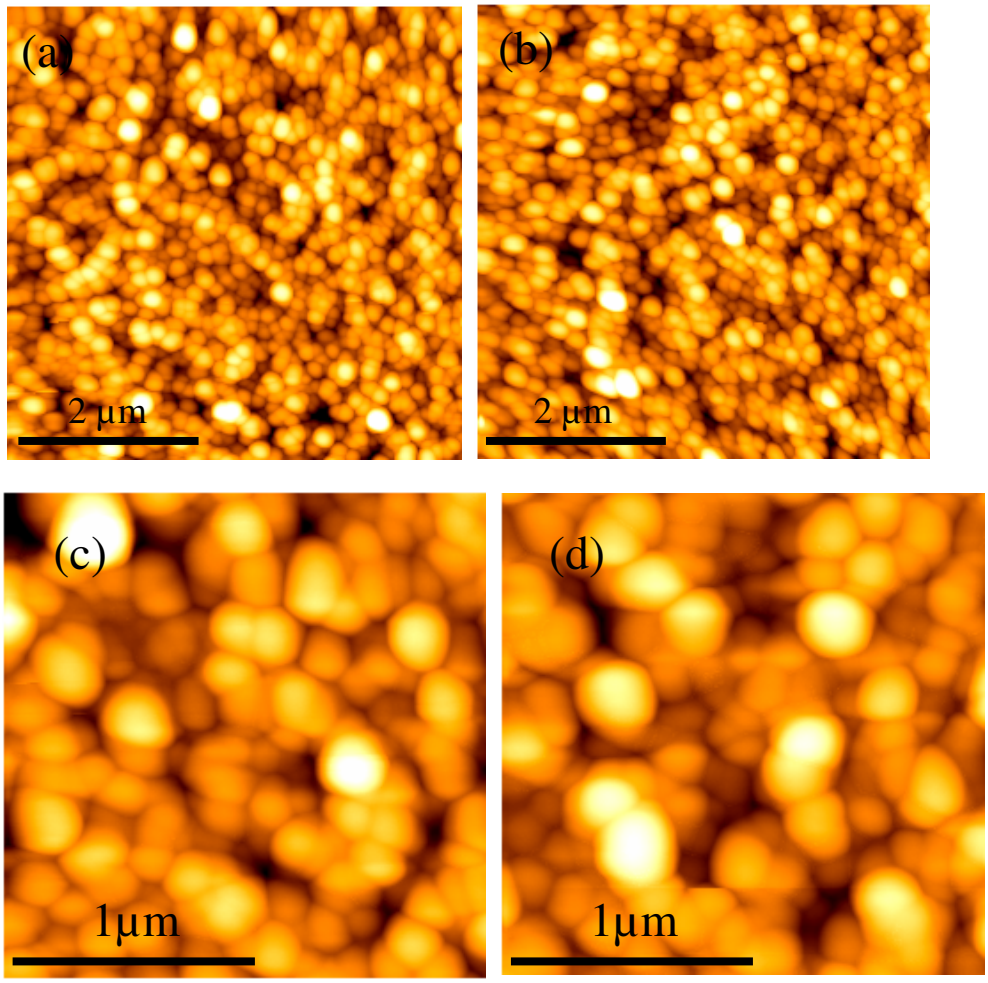

Figure S11. The surface morphology of TiO_2 thin film, for 5 µm windows, annealed at 500 ^{o}C over FQ (a) and SLG (b); for 2 µm windows, annealed at 500 ^{o}C over FQ (c) and SLG (d).

We had observed that the grain size of the film is not much affected by the presence of Na in glass. The AFM images in Figure S11 (a, b for 5 µm window and c, d for 2µm window) show the morphology of films on fused quartz and soda lime glass annealed at 500°C. The average grain sizes are the same within less than about 5%. This supports our conclusion that Na affects the contact of grains rather than the morphology.

This information is available free of charge via the Internet at http://pubs.acs.org.